Vascular tumors in livers with targeted inactivation of the von Hippel–Lindau tumor suppressor

Volker H. Haase*†, Jonathan N. Glickman‡, Merav Socolovsky*, and Rudolf Jaenisch*§¶

*Whitehead Institute for Biomedical Research, Cambridge, MA 02142; †Renal Division, Beth Israel Deaconess Medical Center and Harvard Medical School, Boston, MA 02215; ‡Department of Pathology, Brigham and Women's Hospital and Harvard Medical School, Boston, MA 02115; and §Department of Biology, Massachusetts Institute of Technology, Cambridge, MA 02139

Communicated by Harvey F. Lodish, Massachusetts Institute of Technology, Cambridge, MA, December 6, 2000 (received for review October 27, 2000)

von Hippel–Lindau (VHL) disease is a pleomorphic familial tumor syndrome that is characterized by the development of highly vascularized tumors. Homozygous disruption of the *VHL* gene in mice results in embryonic lethality. To investigate *VHL* function in the adult we have generated a conditional *VHL* null allele (2-*lox* allele) and null allele (1-*lox* allele) by Cre-mediated recombination in embryonic stem cells. We show here that mice heterozygous for the 1-*lox* allele develop cavernous hemangiomas of the liver, a rare manifestation of the human disease. Histologically these tumors were associated with hepatocellular steatosis and focal proliferations of small vessels. To study the cellular origin of these lesions we inactivated *VHL* tissue-specifically in hepatocytes. Deletion of *VHL* in the liver resulted in severe steatosis, many blood-filled vascular cavities, and foci of increased vascularization within the hepatic parenchyma. These histopathological changes were similar to those seen in livers from mice heterozygous for the 1-*lox* allele. Hypoxia-inducible mRNAs encoding vascular endothelial growth factor, glucose transporter 1, and erythropoietin were up-regulated. We thus provide evidence that targeted inactivation of mouse *VHL* can model clinical features of the human disease and underline the importance of the *VHL* gene product in the regulation of hypoxia-responsive genes *in vivo*.

The von Hippel–Lindau (VHL) syndrome is characterized by the dominantly inherited predisposition to develop highly angiogenic tumors. Typically, patients suffer from hemangioblastomas of the retina and central nervous system (CNS), multifocal and bilateral renal cell carcinomas (RCCs), as well as pheochromocytomas (1). Other clinical features include cysts in kidney, liver, and/or pancreas and, in rare cases, vascular tumors of the liver and other non-CNS sites (1–5). The syndrome is caused by germ-line mutations in the *VHL* gene located on chromosome 3p25.5 (6), and tumorigenesis is associated with either the loss or inactivation of the wild-type allele, following Knudson's "two-hit" hypothesis (7–9). *VHL* was also found to be mutated in the majority of sporadic RCCs, as well as in a smaller number of sporadic CNS hemangioblastomas (10–12). On the molecular level, VHL-associated tumors are characterized by the constitutive up-regulation of hypoxia-inducible mRNAs encoding angiogenic growth factors such as vascular endothelial growth factor (VEGF), proteins involved in enhanced glucose metabolism such as glucose transporter 1 (Glut-1), and erythropoietin (Epo) regulating erythropoiesis (13). The *VHL* gene product (pVHL) forms a multimeric protein complex together with Cullin-2, Rbx1, and the Elongins B and C (14–18) and has been shown to negatively regulate hypoxia response genes through ubiquitination of the α-subunit of hypoxia-inducible factor (HIF) (19–21). *VHL* is expressed in most tissues and cell types (6, 22, 23), but relatively little is known about its role in normal organ development.

Homozygous disruption of *VHL* in mice results in embryonic lethality from lack of placental vasculogenesis (24), precluding the investigation of *VHL* function in the adult. We therefore have used conditional gene targeting technology based on Cre-*loxP*-mediated recombination to generate mice in which *VHL* can be inactivated tissue specifically. In this report we present the phenotype resulting from targeted disruption of *VHL* in the liver.

Materials and Methods

Targeting Vector Construction, Generation of Embryonic Stem (ES) Cells, and Mice. Genomic DNA clones containing mouse *VHL* were isolated as *Bam*HI fragments from a 129-mouse-derived P1 library (Genome Systems, St. Louis). A 5-kb *Bam*HI fragment containing exon 1, a 3-kb *Bam*HI fragment containing exon 2, and a 4-kb *Bam*HI fragment containing exon 3 were used to construct the targeting vector BLN-hyTK. The positive–negative selection cassette *loxP*-CMV-hyTK-*loxP* was inserted into an *Nde*I site, 2.6 kb upstream of exon 1. Targeting vector BLN-hyTK was linearized with *Cla*I for electroporation into J1 ES cells. Two hundred ES cell clones were isolated after selection in 140 μg/ml hygromycin (Calbiochem) and analyzed by DNA blot hybridization with an external exon 3 probe. Genomic DNA was digested with *Hin*dIII, allowing screening for the presence of the third l*oxP* site. For the excision of the selection cassette, ES cells were transiently transfected with cytomegalovirus-driven Cre-recombinase (plasmid POG 231, a gift from Stephen O'Gorman, Salk Institute, San Diego). After selection in 2 μM gancyclovir, a total of 400 ES cell clones were analyzed for the presence of a 1-*lox* or 2-*lox* allele by DNA blot hybridization. ES cell DNA was digested with *Nco*I and probed with a 200-bp 5′ *Nde*I–*Apa*I probe. For the generation of chimeras, ES cells heterozygous for a 2-*lox* allele or a 1-*lox* allele were injected into BALB/c blastocysts by standard procedure. Chimeras were bred to BALB/c mice, and germ-line offspring were identified by coat color.

For the generation of mice with liver-specific inactivation of *VHL*, mice homozygous for the 2-*lox* allele were bred to albumin-*cre* transgenic mice (25) that were heterozygous for either the 2-*lox* or the 1-*lox* allele.

Genotyping, RNA, and Protein Analysis. For genotyping of mice, tail DNA was digested with *Nco*I and probed with a 5′ 200-bp *Nde*I–*Apa*I probe. Total RNA was isolated from different mouse tissues with Trizol reagent (GIBCO) according to the manufacturer's instructions. Approximately 20 μg of RNA was size fractionated on 1% denaturing formaldehyde agarose gels. *VHL* mRNA was detected with an exon 3 probe. The VEGF and Glut-1 cDNAs were gifts from Subbian Ananth and Vikas Sukhatme (Beth Israel Deaconess Medical Center), and the

Abbreviations: VHL, von Hippel–Lindau; pVHL, VHL gene product; Epo, erythropoietin; ES, embryonic stem; Glut-1, glucose transporter 1; HIF, hypoxia-inducible factor; PCNA, proliferating cell nuclear antigen; VEGF, vascular endothelial growth factor; RCC, renal cell carcinoma; CNS, central nervous system.

¶To whom reprint requests should be addressed at: Whitehead Institute for Biomedical Research, 9 Cambridge Center, Cambridge, MA 02142. E-mail: jaenisch@wi.mit.edu.

The publication costs of this article were defrayed in part by page charge payment. This article must therefore be hereby marked "*advertisement*" in accordance with 18 U.S.C. §1734 solely to indicate this fact.

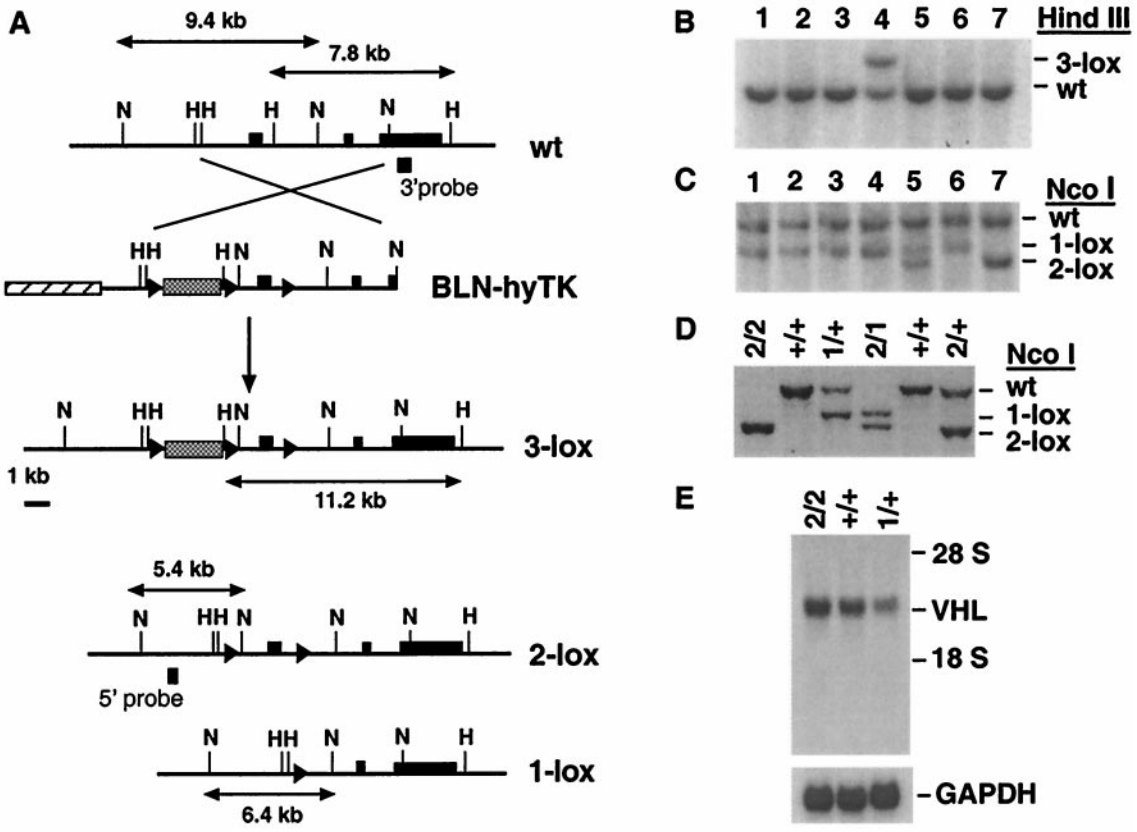

Fig. 1. Generation of mutant mouse lines carrying a conditional *VHL* null allele or null allele. (*A*) Targeting of the murine *VHL* locus with targeting vector BLN-hyTK by homologous recombination. The positive–negative selection cassette CMV-hyTK (stippled box) is flanked by two *loxP* sites (triangles) and was inserted about 2.6 kb upstream of *VHL* exon 1. The third single *loxP* site replaced the *Hin*dIII site in intron 1. Shown is the genomic map of the *VHL* locus before (wt) and after homologous recombination (3-*lox*), as well as the genomic maps of the 2-*lox* and 1-*lox* alleles after Cre-mediated recombination. *VHL* exons 1–3 are depicted by black boxes; the shaded box represents cloning vector pBluescript II. The location of the 5′ and 3′ external probes used in DNA blot analysis is indicated. Abbreviations for restriction sites: H, *Hin*dIII; N, *Nco*I. (*B*) Identification of ES cell clones that have undergone homologous recombination. Detection of both *VHL* wild-type (wt) and 3-*loxP* alleles in ES cell clone 4 and wt allele only in nontargeted ES cell clones by DNA blot analysis. The wt allele is represented by a 7.8-kb fragment, the 3-*loxP* allele by a 11.2-kb fragment. (*C*) Identification of ES cell clones heterozygous for the 2-*lox* or 1-*lox* allele by DNA blot analysis after gancyclovir selection. The 2-*lox* allele is represented by a 5.4-kb fragment, the 1-lox allele by a 6.4-kb fragment. The wt band is 9.4 kb in size. ES cell clone 5 represents a mixed clone. (*D*) Genotype analysis of mice. Abbreviations: 2, 2-*lox* allele; 1, 1-*lox*-allele; +, wild-type allele. (*E*) Comparison of *VHL* mRNA levels between $VHL^{2/2}$ mice and wild-type mice by RNA blot analysis. RNA was isolated from total brain. Glyceraldehyde-3-phosphate dehydrogenase was used as a loading control. Abbreviations are the same as in *D*. The position of ribosomal RNA is indicated.

mouse Epo cDNAs were gifts from Eugene Goldwasser (University of Chicago) and Hong Wu, (University of California, Los Angeles).

Liver whole-cell extracts were prepared by homogenization and lysis in 1% Nonidet P-40, 50 mM Tris (pH 7.4), 150 mM NaCl, 1 mM EDTA, and 15% glycerol, including standard protease inhibitors. Equal amounts of mutant and control liver protein extracts were size separated by 8% SDS-PAGE and transferred to Hybond-C Extra membranes. HIF-2α was detected with a rabbit polyclonal anti-HIF-2α antiserum (Novus Biologicals, Littleton, CO) at a dilution of 1:1,000 and the enhanced chemiluminescence detection system. For the analysis of HIF-1α expression, a monoclonal anti-HIF-1α antibody from Novus Biologicals was used.

Histological Analysis and Electron Microscopy. Tissues were fixed in 10% PBS-buffered formalin or 4% paraformaldehyde and processed for routine embedding in paraffin. Tissues for electron microscopy were fixed in glutaraldehyde. For staining of endothelial cells, 5-μm paraffin-embedded sections were incubated with a rat monoclonal anti-CD31 antibody (PharMingen). Primary antibody was detected with the Vectastain ABC-Elite kit. Diaminobenzidine was used as peroxidase substrate. Staining for proliferating cell nuclear antigen (PCNA) was performed with a commercial kit according to the manufacturer's instructions (Zymed).

Sandwich ELISA for Measurement of Mouse Serum Epo. Plates were coated with monoclonal rat anti-mouse Epo (RDI-MEPOabrt) at 15 μg/ml overnight and blocked in 2% BSA overnight. Mouse serum samples or recombinant mouse Epo (a gift of Amgen, Thousand Oaks, CA) was applied in doubling dilutions in 2% BSA overnight. Bound Epo was detected with a polyclonal rabbit anti-Epo antibody (a gift of Amgen) at 10 μg/ml in 2% BSA for 30 min, followed by an horseradish peroxidase-conjugated goat anti-rabbit IgG (Jackson ImmunoResearch) diluted at 1:15,000 for 30 min. Absorption at 490 nm was measured with a plate reader.

Results

Generation of ES Cells and Mice. For the generation of a conditional null allele (2-*lox* allele), targeting vector BLN-hyTK was constructed. The 2-*lox* allele contains two *loxP* sites, which flank the *VHL* promoter and the first exon (Fig. 1*A*). *Cre*-mediated recombination of the 2-*lox* allele generates a null allele (1-*lox* allele) in which promoter and exon 1 are deleted (Fig. 1*A*). The

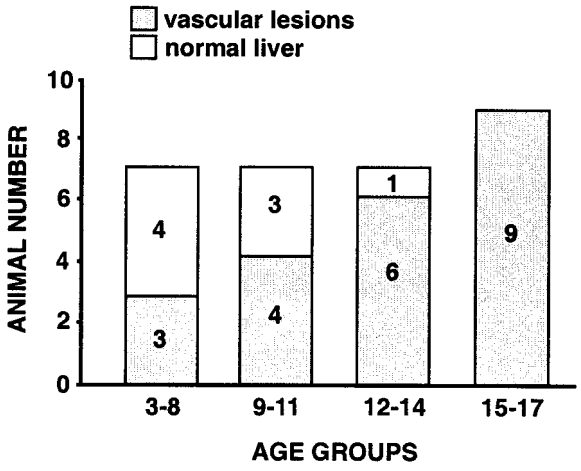

Fig. 2. Incidence of vascular tumors in $VHL^{1/+}$ mice. A total of 30 mice were analyzed. Animals are presented in four age groups. The age is given in months. In the first two groups of animals (age 3–11 months) three mice had small vascular lesions (similar to the lesion seen in Fig. 3*Ab*), and four animals had medium-sized hemangiomas. In the two groups of animals from age 12 to 17 months, seven animals had developed large hemangiomas, three had medium-sized lesions, and five had small lesions.

targeting frequency for vector BLN-hyTK was 1 in 20. A total of five ES cell clones were isolated that carried the 3-*lox* allele (Fig. 1*B*). Four 3-*lox* ES cell clones were independently transfected with Cre-recombinase. After selection in gancyclovir a total of 11 ES cell clones were identified that carried a 2-*lox* allele. The majority of clones isolated were heterozygous for the 1-*lox* allele; some were mixed clones (Fig. 1*C*). Two of the 1-*lox* ES cell clones and two 2-*lox* ES cell clones were injected into BALB/c-derived blastocysts. A total of seven germ-line chimeras were generated (20–70% by coat color).

Mice Homozygous for the 2-*lox* Allele Are Normal. Mice homozygous for the 2-*lox* allele ($VHL^{2/2}$) developed normally and were fertile, suggesting normal expression of this allele, as confirmed by Northern analysis of total brain RNA (Fig. 1*E*). *VHL* mRNA levels in $VHL^{2/2}$ mice were comparable to those seen in wild-type mice ($VHL^{+/+}$), and mRNA levels in mice heterozygous for the 1-*lox* allele ($VHL^{1/+}$) were about half the wild-type level.

Vascular Tumors in Livers from Mice Heterozygous for the 1-*lox* Allele. $VHL^{1/1}$ mice died *in utero* between embryonic days 9 and 11 with a phenotype similar to that previously found (24), whereas $VHL^{1/+}$ mice developed normally and were fertile. However, in contrast to previous studies in which mice heterozygous for *VHL* disruption were found to have no phenotype at 15 months of age (24), animals heterozygous for the 1-*lox* mutation developed cavernous hemangiomas in their livers (22/30), with an increase in incidence at older age (Fig. 2), and very rarely single renal cysts (1/30). Vascular lesions were seen in more than 90% of mice between the ages of 12 and 17 months, whereas only 50% of mice between the ages of 3 and 12 months were affected (Fig. 2). This finding indicates that animals heterozygous for a *VHL* gene deletion are predisposed to develop vascular tumors similar to human carriers of *VHL* germ-line mutations. In contrast to patients with VHL syndrome, vascular tumors were observed in the liver only, whereas renal cysts were extremely rare, and RCC, adrenal, and pancreatic tumors were not found.

The vascular tumors ranged from small (Fig. 3*A b* and *c*) to large cavernous hemangiomas (Fig. 3*Aa*), which in extreme cases affected the entire liver. Histologically we found large vascular cavities (Fig. 3 *Ae* and *B*) that were associated with hepatocellular steatosis (Fig. 3*B*), focal proliferations of small vessels, and spindle cells that stained positive for the proliferation marker PCNA (Fig. 3 *C* and *D*). The endothelial nature of cells lining the small vessels and cavities was confirmed by immunostaining for CD31 (Fig. 3 *Af* and *D*). Some of the spindle cells also stained positive for CD31 (not shown here), suggesting that these cells may represent endothelial precursor cells (26).

VHL-associated tumors frequently show loss of heterozygosity, indicating loss of the wild-type allele. Thus far we have not been able to demonstrate loss of heterozygosity conclusively in microscopically dissected $VHL^{1/+}$ vascular lesions with the use of several mouse chromosome 6 polymorphic markers (data not shown here).

Phenotypic Analysis of Albumin-*cre* Mutant Mice. Because *VHL* gene mutations have been found in the nonendothelial component of human CNS hemangioblastomas (12, 27), we speculated that inactivation or loss of the normal *VHL* allele in hepatocytes rather than in liver endothelial cells may have led to the development of vascular tumors in $VHL^{1/+}$ mice. To test this hypothesis we inactivated *VHL* in hepatocytes by crossing $VHL^{2/2}$ mice with albumin-*cre* transgenic mice (25). Loop-out efficiency in the liver was estimated to be between 40% and 60% by DNA blot analysis and was limited to the liver at the age of 3 months.

Albumin-*cre* mutants developed severe hepatomegaly, were runt (about half the weight of littermate controls), appeared sick, and died between the ages of 6 and 12 weeks. Although mutants did not develop the large cavernous hemangiomas found in $VHL^{1/+}$ mice, their livers shared many histological features, such as hepatocellular steatosis, numerous blood-filled vascular cavities, and foci of increased vascularization within the hepatic parenchyma (Fig. 3*B*). Larger lesions were not seen in these mice because development of large vascular cavities probably requires time and mutants died at a young age. Significant hepatic steatosis was detectable by 2 weeks of age. Vascular lesions became obvious between 4 and 6 weeks of age. Hepatic steatosis was due to the accumulation of neutral fat in hepatocytes, as documented by a positive oil red O stain (not shown here) and electron microscopy (Fig. 3*C*). Similar lipid accumulation has also been found in the stromal cell component of CNS hemangioblastomas, which has been shown to undergo *VHL* inactivation (12, 27, 28). Our data demonstrate that *VHL* inactivation in hepatocytes can reproduce the histological features of vascular lesions found in $VHL^{1/+}$ mice and further suggest that lipid accumulation is a direct consequence of *VHL* inactivation.

Molecular Analysis of Albumin-*cre* Mutant Mice. pVHL-deficient cell lines have been shown to stabilize the α-subunits of HIF-1 and HIF-2, thereby up-regulating hypoxia-responsive mRNAs, such as those encoding VEGF and Glut-1 (19). We therefore quantitated VEGF and Glut-1 mRNA levels in mutant livers by RNA blot analysis. VEGF as well as Glut-1 mRNA levels were abundant in mutant livers but hard to detect in livers from littermate controls (Fig. 4*B*). These data are consistent with previous findings in human hemangioblastomas (29, 30). HIF-2α was readily detectable in albumin-*cre* mutant livers by Western blot analysis but was absent from control tissue (Fig. 4*C*). However, we were unable to detect HIF-1α in mutant livers or control livers from anemic animals with the currently available immunological reagents. Our findings suggest that the vascular changes seen in *VHL*-deficient livers may result in part from the inability to properly regulate the activity of HIF-2 and VEGF.

Polycythemia and Elevated Serum Epo Levels in Albumin-*cre* Mutants. Because VHL-associated tumors have been shown to secrete Epo (29) we measured complete blood counts in albumin-*cre*

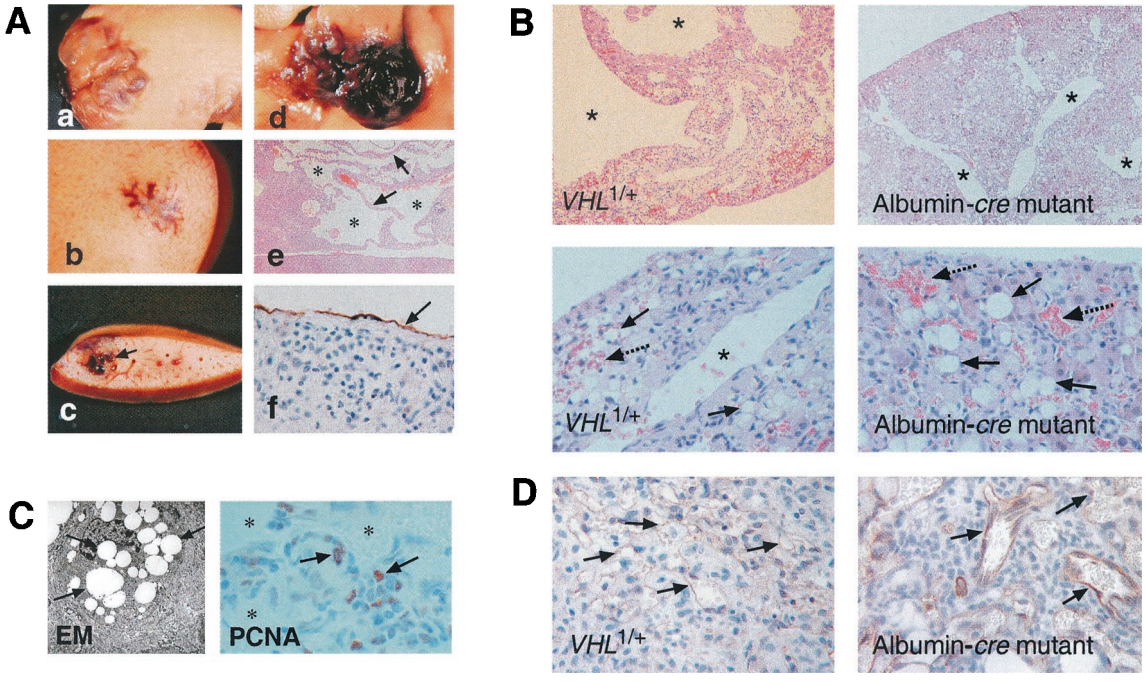

Fig. 3. Spectrum of vascular tumors found in livers of $VHL^{1/+}$ mice and histological comparison of $VHL^{1/+}$ vascular lesions with vascular lesions found in albumin-*cre* mutant livers. (*A*) Livers were fixed in formalin before gross photography. (*a*) Gross photograph of a large cavernous hemangioma of the right liver lobe. (*b*) Gross photograph of a small vascular lesion in unsectioned liver. (*c*) Liver from *Ab* sectioned. The vascular lesion is indicated by the arrow. (*d*) Example of a medium-sized hemangioma of the right liver lobe. (*e*) Paraffin section of a cavernous hemangioma stained with H&E. The arrows point to cords of normal-appearing hepatocytes; stars depict vascular cavities. (*f*) CD31 immunostain of endothelial cells lining a large cavity. (*B*) Comparison of $VHL^{1/+}$ with albumin-*cre* vascular lesions at low-power and high-power magnification. Stars indicate endothelium-lined vascular spaces. Straight arrows point to lipid-containing hepatocytes. Small vascular spaces/vessels are indicated by dashed arrows. (*C*) Analysis of hepatocellular lipid vacuoles by electron microscopy, and PCNA staining of $VHL^{1/+}$ vascular liver lesions. Shown on the left is a hepatocyte containing multiple lipid vacuoles (arrows), the appearance of which is consistent with neutral lipid (triglyceride). Shown on the right are PCNA-positive cells (arrows) in a typical vascular lesion; small vessels are marked with stars. (*D*) Foci of increased vascularization in $VHL^{1/+}$ and albumin-*cre* mutant livers and CD31 immunostain of small vessels (arrows).

mutants and in $VHL^{1/+}$ mice. We found that albumin-*cre* mutants developed erythrocytosis (Fig. 5*A*), whereas $VHL^{1/+}$ mice affected by cavernous hemangiomas had normal blood counts (not shown). The difference in blood counts is probably a reflection of the number of hepatocytes that have undergone homozygous *VHL* inactivation. Whereas at least 40–60% of all hepatocytes in albumin-*cre* mutants lack *VHL*, a much smaller number are affected in heterozygotes, as vascular lesions are localized and associated hepatocellular steatosis is focal. To rule out a primary cause for polycythemia, we measured serum Epo levels by ELISA. Serum Epo levels were increased (Fig. 5*B*), as were Epo mRNA levels in mutant livers (data not shown). These findings demonstrate that erythrocytosis in albumin-*cre* mutants is secondary to increased serum Epo levels and does not result from a primary process. The Epo levels in mutants were estimated to be 100 and 200 milliunits/ml. The normal serum Epo concentration range is 10–30 milliunits/ml. We suggest that inactivation of *VHL* in hepatocytes leads to ectopic Epo secretion from these cells.

Discussion

Here we provide evidence that clinical features of VHL disease can be reproduced by targeted mutagenesis of *VHL* in the laboratory mouse. Our findings demonstrate that mice heterozygous for a *VHL* null mutation are susceptible to the development of spontaneous vascular tumors. This susceptibility is reminiscent of the autosomal dominantly inherited predisposition of VHL patients to tumorigenesis. The discrepancy between our observation and the previously reported findings in heterozygous *VHL* knockout mice (24) may be a result of differences in genetic background. It is well established that differences in genetic background can account for variable phenotypic penetrance of targeted null mutations (31). In contrast to the pleomorphic nature of the human disease, the tumor spectrum and location in mice were restricted to cavernous hemangiomas of the liver. We speculate that in $VHL^{1/+}$ mice, hepatocytes are particularly susceptible to loss or inactivation of their wild-type *VHL* allele. We performed PCR-based studies to assess vascular lesions for loss of heterozygosity but have not been able to demonstrate loss of heterozygosity conclusively, probably because of the high degree of cellular heterogeneity in these lesions. It is plausible, however, that the remaining wild-type allele has been inactivated by a different molecular mechanism, such as transcriptional silencing through hypermethylation. Hypermethylation of a 5′ CpG island in the *VHL* gene has been shown to be an important mechanism for *VHL* inactivation in a significant number of RCC cases, where mutations in the remaining *VHL* allele could not be found (7). On the other hand, vascular lesions in $VHL^{1/+}$ livers could be due to haploinsufficiency, leading to increased VEGF production by a subgroup of liver cells, in which pVHL is normally less abundant. However, there is currently no experimental evidence for such normally occurring variability in cellular pVHL levels.

Furthermore, it remains unclear why vascular tumors in mice occurred in the liver only and why, in contrast to humans, other VHL-associated tumors such as RCC could not be found. It is possible that the development of RCCs in $VHL^{1/+}$ heterozygotes may require additional mutations in other tumor suppressor genes (32).

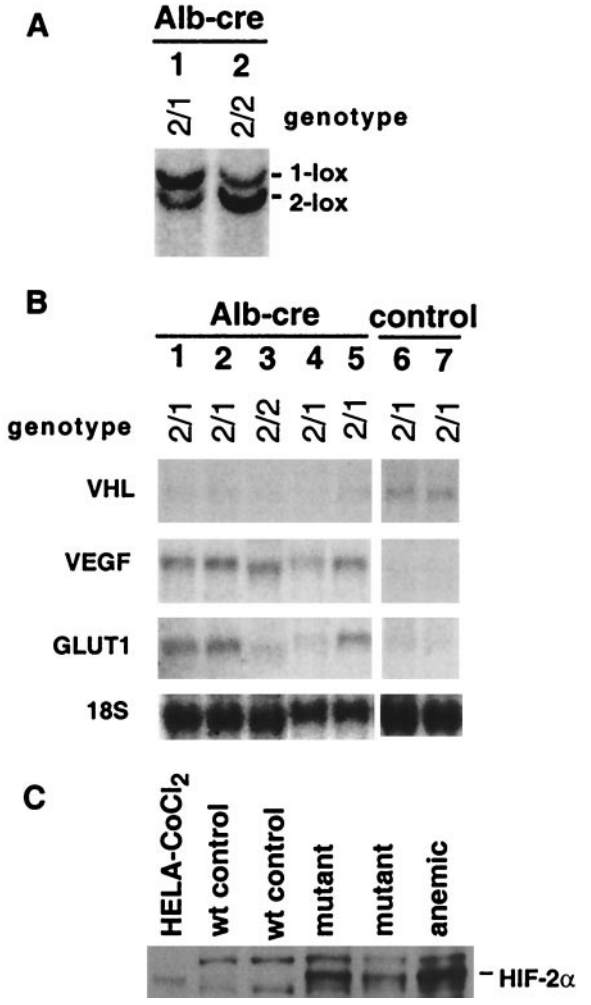

Fig. 4. Molecular analysis of albumin-*cre* mutant livers. (*A*) DNA blot analysis of two albumin-*cre* mutant livers. The genotype as determined by tail DNA analysis is indicated. Note the appearance of a new band (1-*lox* allele) in lane 2 and a shift in the ratio of the two bands toward the 1-*lox* allele in lane 1, indicating albumin-*cre* mediated recombination. (*B*) Analysis of VHL target gene expression by RNA blot. Lanes 1–5 represent total RNA samples from mutant livers; lanes 6 and 7 are controls. (*C*) HIF-2α expression in mutant livers. HIF-2α is detected in mutant livers and absent from wild-type control livers. The two nonspecific background bands were found in all mouse samples and are not present in the human sample. Whole-cell protein extracts from $CoCl_2$-treated HELA cells and an anemic mouse liver were used as positive controls. The mouse HIF-2α protein is slightly larger than the human homologue (37), hence the small difference in migration between the two species.

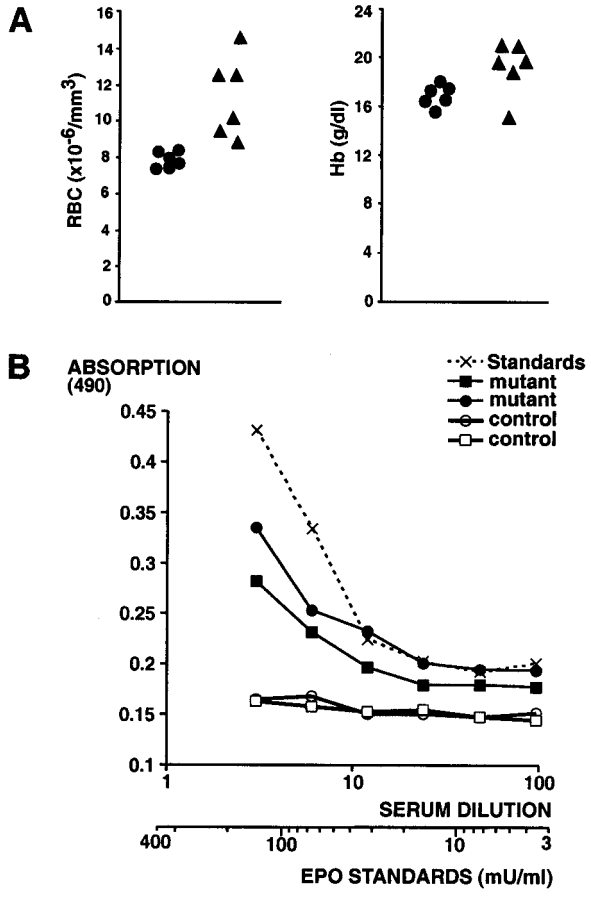

Fig. 5. Albumin-*cre* mutants develop polycythemia secondary to elevated serum Epo levels. (*A*) Red blood cell (RBC) number and hemoglobin concentration in blood from 2-month-old mice were analyzed with a Hemavet counter. ●, Values for age-matched controls (total of six); ▲, values for albumin-*cre* mutants (total of six). (*B*) Raised serum Epo in albumin-*cre* mutants. A sandwich ELISA assay was used to measure serum Epo concentration. Mouse serum samples were diluted as indicated in 2% BSA and applied to the plates. Recombinant mouse Epo diluted in 2% BSA was used for the standard curve.

VHL-deficient hepatocytes accumulate neutral lipids, resulting in a clear cell morphology. Lipid accumulation and/or clear cell morphology is a common histological finding in VHL-associated tumors, for instance in the stromal cells of hemangioblastomas and the tumor cells of VHL-associated RCC. The biochemical basis for this phenomenon is unclear but could conceivably reflect HIF-dependent alterations in carbohydrate or triglyceride metabolism.

VHL$^{1/+}$ mice and albumin-*cre* mutants develop similar vascular histopathologies. VEGF mRNA levels are strongly upregulated in albumin-*cre* mutant livers. VEGF is a very potent mitogen for endothelial cells and is critically important for vasculogenesis, angiogenesis, and maintenance of existing blood vessels (26). Because VEGF mRNA levels are high in albumin-*cre* mutant livers, we suggest that the observed vascular lesions are a result of abnormal VEGF production in hepatocytes. *VEGF* and other hypoxia response genes such as *Epo* and *Glut-1* are transcriptionally regulated by the heterodimeric basic helix—loop–helix transcription factor HIF. Degradation of the HIF α-subunit normally depends on tissue oxygen tension, except in *VHL*-deficient RCC cell lines, in which HIF-α is constitutively stabilized (19). It has been shown recently that pVHL is part of a multimeric protein complex that has ubiquitin ligase activity and targets the α-subunit of HIF-1 and -2, leading ultimately to the degradation of HIF-α by the proteasome (20, 21). We show here that elevated HIF-2α levels can be found in *VHL*-deficient livers. This finding suggests that pVHL could act as a regulator of HIF-2α stability in tissues other than renal cancer and points to a more general role of pVHL in the regulation of HIF-α.

Albumin-*cre* mutant mice develop polycythemia from increased Epo production in the liver. Polycythemia can be observed in up to 20% of patients with capillary hemangioblastomas, and elevated Epo mRNA levels have been found in hemangioblastomas and renal cell cancers (29, 30, 33). Liver Epo mRNA levels have previously been shown to be increased in rodents treated with $CoCl_2$, a hypoxia mimetic (34). Besides its role in erythropoiesis, Epo has been shown to be an angiogenic

growth factor (35, 36) and may, in concert with VEGF, play a significant role in the pathogenesis of the vascular lesions found in *VHL*-deficient livers.

In summary, we provide evidence that clinical features of VHL disease can be modeled by targeted inactivation of *VHL* in the laboratory mouse. The molecular analysis of albumin-*cre* mutant livers suggests that inactivation of *VHL* leads to the up-regulation of VEGF, Glut-1, and Epo mRNAs, as well as stabilization of HIF-2α in hepatocytes. These findings underline the importance of pVHL as a negative regulator of hypoxia-inducible genes *in vivo* and argue for a general role of pVHL in the regulation of HIF activity.

We thank Jessica Dausman and Ruth Flannery for help with mice; Jeanne Reis for preparing tissue sections; Mark Magnuson for providing the albumin-*cre* transgenic line; and Schahram Akbarian, Anton Wutz, and other members of the Jaenisch laboratory for helpful discussions and suggestions. This work was supported by grants from the National Cancer Institute (5-R35-CA44339) to R.J. and the National Institute of Diabetes and Digestive and Kidney Diseases (K08-DK02668) to V.H.H.

1. Maher, E. R. & Kaelin, W. G., Jr. (1997) *Medicine (Baltimore)* **76,** 381–391.
2. Burns, C., Levine, P. H., Reichman, H. & Stock, J. L. (1987) *Am. J. Med. Sci.* **293,** 119–121.
3. Rojiani, A. M., Owen, D. A., Berry, K., Woodhurst, B., Anderson, F. H., Scudamore, C. H. & Erb, S. (1991) *Am. J. Surg. Pathol.* **15,** 81–86.
4. McGrath, F. P., Gibney, R. G., Morris, D. C., Owen, D. A. & Erb, S. R. (1992) *Clin. Radiol.* **45,** 37–39.
5. Neumann, H. P. & Zbar, B. (1997) *Kidney Int.* **51,** 16–26.
6. Latif, F., Tory, K., Gnarra, J., Yao, M., Duh, F. M., Orcutt, M. L., Stackhouse, T., Kuzmin, I., Modi, W., Geil, L., *et al.* (1993) *Science* **260,** 1317–1320.
7. Herman, J. G., Latif, F., Weng, Y., Lerman, M. I., Zbar, B., Liu, S., Samid, D., Duan, D. S., Gnarra, J. R., Linehan, W. M., *et al.* (1994) *Proc. Natl. Acad. Sci. USA* **91,** 9700–9704.
8. Richards, F. M., Crossey, P. A., Phipps, M. E., Foster, K., Latif, F., Evans, G., Sampson, J., Lerman, M. I., Zbar, B., Affara, N. A., *et al.* (1994) *Hum. Mol. Genet.* **3,** 595–598.
9. Crossey, P. A., Foster, K., Richards, F. M., Phipps, M. E., Latif, F., Tory, K., Jones, M. H., Bentley, E., Kumar, R., Lerman, M. I., *et al.* (1994) *Hum. Genet.* **93,** 53–58.
10. Gnarra, J. R., Tory, K., Weng, Y., Schmidt, L., Wei, M. H., Li, H., Latif, F., Liu, S., Chen, F., Duh, F. M., *et al.* (1994) *Nat. Genet.* **7,** 85–90.
11. Foster, K., Prowse, A., van den Berg, A., Fleming, S., Hulsbeek, M. M., Crossey, P. A., Richards, F. M., Cairns, P., Affara, N. A., Ferguson-Smith, M. A., *et al.* (1994) *Hum. Mol. Genet.* **3,** 2169–2173.
12. Lee, J. Y., Dong, S. M., Park, W. S., Yoo, N. J., Kim, C. S., Jang, J. J., Chi, J. G., Zbar, B., Lubensky, I. A., Linehan, W. M., *et al.* (1998) *Cancer Res.* **58,** 504–508.
13. Iliopoulos, O., Levy, A. P., Jiang, C., Kaelin, W. G., Jr. & Goldberg, M. A. (1996) *Proc. Natl. Acad. Sci. USA* **93,** 10595–10599.
14. Pause, A., Lee, S., Worrell, R. A., Chen, D. Y., Burgess, W. H., Linehan, W. M. & Klausner, R. D. (1997) *Proc. Natl. Acad. Sci. USA* **94,** 2156–2161.
15. Kamura, T., Koepp, D. M., Conrad, M. N., Skowyra, D., Moreland, R. J., Iliopoulos, O., Lane, W. S., Kaelin, W. G., Jr., Elledge, S. J., Conaway, R. C., *et al.* (1999) *Science* **284,** 657–661.
16. Stebbins, C. E., Kaelin, W. G., Jr. & Pavletich, N. P. (1999) *Science* **284,** 455–461.
17. Kibel, A., Iliopoulos, O., DeCaprio, J. A. & Kaelin, W. G., Jr. *(1995) Science* **269,** 1444–1446.
18. Duan, D. R., Pause, A., Burgess, W. H., Aso, T., Chen, D. Y., Garrett, K. P., Conaway, R. C., Conaway, J. W., Linehan, W. M. & Klausner, R. D. (1995) *Science* **269,** 1402–1406.
19. Maxwell, P. H., Wiesener, M. S., Chang, G. W., Clifford, S. C., Vaux, E. C., Cockman, M. E., Wykoff, C. C., Pugh, C. W., Maher, E. R. & Ratcliffe, P. J. (1999) *Nature (London)* **399,** 271–275.
20. Cockman, M. E., Masson, N., Mole, D. R., Jaakkola, P., Chang, G. W., Clifford, S. C., Maher, E. R., Pugh, C. W., Ratcliffe, P. J. & Maxwell, P. H. (2000) *J. Biol. Chem.* **275,** 25733–25741.
21. Ohh, M., Park, C. W., Ivan, M., Hoffman, M. A., Kim, T. Y., Huang, L. E., Pavletich, N., Chau, V. & Kaelin, W. G. (2000) *Nat. Cell Biol.* **2,** 423–427.
22. Kessler, P. M., Vasavada, S. P., Rackley, R. R., Stackhouse, T., Duh, F. M., Latif, F., Lerman, M. I., Zbar, B. & Williams, B. R. (1995) *Mol. Med.* **1,** 457–466.
23. Richards, F. M., Schofield, P. N., Fleming, S. & Maher, E. R. (1996) *Hum. Mol. Genet.* **5,** 639–644.
24. Gnarra, J. R., Ward, J. M., Porter, F. D., Wagner, J. R., Devor, D. E., Grinberg, A., Emmert-Buck, M. R., Westphal, H., Klausner, R. D. & Linehan, W. M. (1997) *Proc. Natl. Acad. Sci. USA* **94,** 9102–9107.
25. Postic, C., Shiota, M., Niswender, K. D., Jetton, T. L., Chen, Y., Moates, J. M., Shelton, K. D., Lindner, J., Cherrington, A. D. & Magnuson, M. A. (1999) *J. Biol. Chem.* **274,** 305–315.
26. Carmeliet, P. (2000) *Nat. Med.* **6,** 389–395.
27. Vortmeyer, A. O., Gnarra, J. R., Emmert-Buck, M. R., Katz, D., Linehan, W. M., Oldfield, E. H. & Zhuang, Z. (1997) *Hum. Pathol.* **28,** 540–543.
28. Lach, B., Gregor, A., Rippstein, P. & Omulecka, A. (1999) *Ultrastruct. Pathol.* **23,** 299–310.
29. Krieg, M., Marti, H. H. & Plate, K. H. (1998) *Blood* **92,** 3388–3393.
30. Wizigmann-Voos, S., Breier, G., Risau, W. & Plate, K. H. (1995) *Cancer Res.* **55,** 1358–1364.
31. LeCouter, J. E., Kablar, B., Whyte, P. F., Ying, C. & Rudnicki, M. A. (1998) *Development (Cambridge, UK)* **125,** 4669–4679.
32. Martinez, A., Fullwood, P., Kondo, K., Kishida, T., Yao, M., Maher, E. R. & Latif, F. (2000) *Mol. Pathol.* **53,** 137–144.
33. Da Silva, J. L., Lacombe, C., Bruneval, P., Casadevall, N., Leporrier, M., Camilleri, J. P., Bariety, J., Tambourin, P. & Varet, B. (1990) *Blood* **75,** 577–582.
34. McDonald, J. D., Lin, F. K. & Goldwasser, E. (1986) *Mol. Cell. Biol.* **6,** 842–848.
35. Ribatti, D., Presta, M., Vacca, A., Ria, R., Giuliani, R., Dell'Era, P., Nico, B., Roncali, L. & Dammacco, F. (1999) *Blood* **93,** 2627–2636.
36. Anagnostou, A., Lee, E. S., Kessimian, N., Levinson, R. & Steiner, M. (1990) *Proc. Natl. Acad. Sci. USA* **87,** 5978–5982.
37. Tian, H., McKnight, S. L. & Russell, D. W. (1997) *Genes Dev.* **11,** 72–82.